



# Senescence-unrelated impediment of osteogenesis from Flk1<sup>+</sup> bone marrow mesenchymal stem cells induced by total body irradiation and its contribution to long-term bone and hematopoietic injury

Jie Ma, Mingxia Shi, Jing Li, Bin Chen, Honglan Wang, Bingzong Li, Jianli Hu, Ying Cao, Baijun Fang, Robert Chunhua Zhao

From the Institute of Basic Medical Sciences and School of Basic Medicine, Center of Excellence in Tissue Engineering, Chinese Academy of Medical Sciences and Peking Union Medical College, Beijing, 100005, China

Funding: this work was supported by grants from the "863 Projects" of the Ministry of Science and Technology of PR China (No. 2002AA205061); the Beijing Ministry of Science and Technology (No. 2002-489); the China Medical Board of New York, Stem Cell Biology, Engineering (No. 01-748); and the National Natural Science Foundation of China (No. 30570771, No. 30125018). R.C.H. Zhao is a Cheung Kong Scholar in RP China.

Acknowledgments: we thank Hengjiang Cai of the department of orthopaedics of Beijing Hospital for help with the bone mineral density analysis and Jane Qiu for revising the manuscript.

Manuscript received December 5, 2006.  
Manuscript accepted April 30, 2007.

Correspondence:  
Robert Chunhua Zhao, M.D., Ph.D.,  
Professor of the Institute of Basic  
Medical Sciences and School of  
Basic Medicine, Director of the  
Center for Tissue Engineering,  
Chinese Academy of Medical  
Sciences and Peking Union Medical  
College, 5 Dongdangantiao, Beijing  
100005, P.R. China.  
E-mail: chunhuaz@public.tpt.tj.cn

## ABSTRACT

### Background and Objectives

Ionizing irradiation is a common treatment for cancer patients and can result in adverse side effects affecting the bone and hematopoietic systems. Although some studies have demonstrated that ionizing radiation can induce apoptosis and senescence in hematopoietic stem cells, little is known about the effects of total body irradiation (TBI) on bone marrow (BM) mesenchymal stem cells (MSC). The objectives of this study were to determine the response of BM MSC to irradiation stress, such as cellular senescence and differentiation potential, and the clinical significance of these changes caused by TBI.

### Design and Methods

At different time points after TBI, Flk1<sup>+</sup> MSC were isolated from BM of male C57BL/6 mice and analyzed for colony forming units-fibroblast (CFU-F), cellular senescence-related indices and osteogenic potential. Bone histomorphometric analysis, immunohistochemical staining and bone mineral density (BMD) tests were performed to detect the effects of TBI on bone and the hematopoietic system.

### Results

TBI reduced the pool of BM mesenchymal stem/progenitor cells, and altered osteoblast differentiation ability of BM MSC, evidenced by changes in TAZ expression. These alterations, sustained up to 28 days post-irradiation, were independent of cellular senescence in BM MSC. Irradiated mice showed obvious bone loss and destruction of the hematopoietic osteoblastic niche, which normally comprise of spindle-shaped N-cadherin-expressing osteoblasts.

### Interpretation and Conclusions

TBI treatment results in impairment in BM MSC, which might be responsible for bone loss and, at least partially, for impaired hematopoiesis.

Key Words: total body irradiation, mesenchymal stem cells, senescence, osteogenesis, bone and hematopoietic injury.

Haematologica 2007; 92:889-896

©2007 Ferrata Storti Foundation

**I**onizing irradiation is a common treatment for cancer patients. Despite its therapeutic value, the adverse side effects can be significant. It has been well established that ionizing radiation can result in acute myelosuppression by inducing apoptosis of hematopoietic cells,<sup>1,2</sup> and cause long-term residual damage to bone marrow (BM) hematopoietic function as manifested by a defect in hematopoietic stem cell (HSC) self-renewal and a decrease in HSC reserves.<sup>3,4</sup> The residual BM damage is latent but long-lasting, and shows little tendency to recover. Evidence from both *in vitro* culture systems and murine models has indicated that HSC senescence – a complex phenotype characterized by reduced repair and/or regeneration of lost or damaged cells – may be the underlying cause of the long-term residual damage to BM hematopoietic function.<sup>5,6</sup>

In addition to the roles of HSC, the initiation and maintenance of hematopoiesis also depends on the hematopoietic microenvironment or niche, which ensures the size of the stem cell pool and regulates the differentiation of HSC. BM mesenchymal stem cells (MSC) are non-hematopoietic stem cells, which also reside in the bone cavity and can give rise to chondrocytes, osteoblasts, fibroblasts, adipocytes, and endothelial cells, some of which are the cellular components of the hematopoietic niche.<sup>7-9</sup> BM MSC also have the potential to participate in endogenous tissue regeneration and organ repair, especially in response to disease or injury. Therefore, it is plausible that the induction of BM MSC senescence could contribute significantly to the long-term tissue injury induced by ionizing radiation, not only including the residual damage to the hematopoietic system but also other related systems given the multi-lineage differentiating capacity of these cells. In addition, although it has been reported that allogeneic bone marrow transplantation conditioning with high-dose chemotherapy and total body irradiation (TBI) causes irreversible depletion of colony-forming units-fibroblasts (CFU-F) and a 20% loss of BMD,<sup>10</sup> the specific effect of ionizing radiation on BM MSC is still not determined. In this study, we used a murine TBI model to examine the impact of TBI on BM MSC, and its relevance to clinical manifestations of TBI-related bone loss. We also tried to determine whether the hematopoietic niche is impaired as a result of ionizing radiation.

## Design and Methods

### Animals

Male C57BL/6 mice aged 5 weeks were purchased from the Experimental Animal Institute of the Chinese Academy of Medical Sciences (Beijing, China). All the animal handling and experimental procedures were approved by the Animal Care and Use Committee of the Chinese Academy of Medical Sciences.

### Ionizing radiation

The mice were exposed, on a rotating platform, to a single challenge of 4 Gy TBI in a <sup>137</sup>cesium gamma-irradiator

(Gammacell 40, CES IUM 137, Atomic Energy of Canada Limited Radiochemical Inc., Ottawa, Ontario, Canada) at a rate of 2.4 Gy/min.

### Isolation of Flk1+ murine MSC

Flk1<sup>+</sup> murine MSC from the BM of male C57BL/6 were isolated using previously described methods.<sup>11,12</sup> The main phenotype of these cells was persistently CD34, CD45, CD31, vWF, GlyA, CD11a, CD11b negative, and Flk1 positive (*data not shown*). We, therefore, termed them Flk1<sup>+</sup> murine MSC. In this study, BM MSC isolated from the mice 1, 3, 7, 14 and 28 days after TBI are named D1, D3, D7, D14, and D28, respectively. The BM MSC from normal mice are denoted as D0.

### Bone marrow CFU-F assay

Bone marrow mononuclear cells (BM MNC) (5×10<sup>6</sup>) from unirradiated mice and mice at different time points after TBI were isolated and cultured in T25 flasks with MSC culture medium. Half the medium was refreshed every 3 days and cultures were stopped on day 9. The medium was then removed and the flasks were washed twice with phosphate-buffered saline (PBS), fixed with methanol, and stained with Crystal violet. The fibroblast colonies were counted using an inverted microscope at 100× magnification. Cell clusters consisting of at least 50 fibroblasts were scored as a CFU-F colony.

### Cell cycle analysis

BM MSC were trypsinized, fixed overnight with 75% cold ethanol, and labeled with 50 µg/mL propidium iodide (Sigma) and 20 µg/mL Rnase A for 30 min at 37°C. DNA content was analyzed in a FACScan flow cytometer (Beckton-Dickinson, San José, CA, USA) with ModFit LT software.

### Senescence-associated β-galactosidase (SA-β-gal) activity analysis

SA-β-gal activity in cultured BM MSC isolated from mice which had or had not undergone TBI was determined using a SA-β-gal staining kit (Cell Signaling Technology, Beverly, MA, USA) according to the manufacturer's instructions. Senescent cells were identified as blue-stained cells by standard light microscopy. A total of 1000 cells were counted in five random fields in a well to determine the percentage of SA-β-gal positive cells.

### In vitro osteogenic differentiation, alkaline phosphatase (ALP) and calcium assays

Osteogenic differentiation was induced as previously described.<sup>12</sup> One week later, ALP histochemistry was performed using an ALP kit (Institute of Hematology and Blood Diseases Hospital, CAMS & PUMC) as recommended by the manufacturer. After inductive differentiation *in vitro* for 3 weeks, calcium accumulation was measured by Von Kossa staining.<sup>12</sup>

### Real-time reverse transcriptase analysis

Total RNA isolation, preparation of cDNA, and real-time quantitative RT-PCR were performed as previously described.<sup>13,14</sup> The sequences of primers and their specific annealing temperature are presented in *Supplementary Table 1*. All experiments were performed at least three times.

### Bone histomorphometric analysis

The femora collected from mice that had or had not received TBI were fixed in phosphate-buffered 10% formalin (pH 7.4). To examine the osteoblasts and osteoid, samples were left undecalcified, dehydrated, infiltrated and embedded in methyl methacrylate. For regular histomorphometry, the femora were decalcified in 15% EDTA for 1 week, dehydrated in progressive concentrations of ethanol, cleared in xylene, and embedded in paraffin. The entire femur was then sectioned longitudinally in 5 µm sections, stained with toluidine blue and hematoxylin and eosin (HE). The osteoblast quantitative analysis was performed using the method described by Zhang<sup>15</sup> with minor alterations. Both oval-shaped and spindle-shaped osteoblasts in one section were counted in a blind fashion.

### Immunohistochemical staining

The paraffin-embedded femoral sections were prepared as described above. Staining for N-cadherin was performed with rabbit polyclonal antibody to N-cadherin antibody (Abcam, Cambridge, CA, USA), diluted 1:200, along with the following procedure recommended by the manufacturer of the streptavidin/peroxidase Histostain™-Plus Kits (Zymed, San Francisco, USA). For quantitative analysis of N-cadherin<sup>+</sup> cells, three people counted the spindle-shaped N-cadherin-expressing osteoblasts (SNO) in these sections in a blind fashion.<sup>15</sup>

### BMD measurements

Dual-energy X-ray absorptiometry (DEXA) was performed on a LEXXOS DIGITAL 2D DENSITOMETER (Diagnostic Medical System [DMS], Montpellier, France) that was calibrated daily as suggested by the manufacturer. Each set of animal scans was preceded by scanning a plastic embedded murine phantom. After induction of anesthesia with 120 µg/10 g body weight sodium pentobarbital i.p., mice were placed on the imaging-positioning tray in a prostrate position. BMD was measured with a

**Table 1.** TBI-induced cell cycle alteration of BM MSC.

	D0	D3	D7	D28
G0/G1	86.1±2.64	74.07±1.31*	81.09±2.21	85.06±2.31
S	5.38±1.33	12.55±1.86*	8.15±1.01*	7.44±0.22
G2/M	8.49±3.66	13.37±3.07	10.76±1.20	7.45±2.28

Cell cycle analysis of BM MSC derived from irradiated (D3, D7 and D28) and unirradiated mice (D0) was performed as indicated in the Design and Methods section. Data represent means±SD of three independent experiments. \* $p < 0.05$  vs. D0

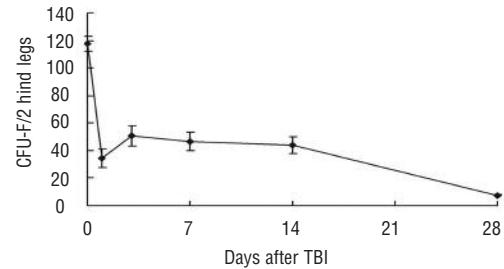


**Figure 1.** TBI caused shrinkage of the BM mesenchymal stem/progenitor cell pool.  $5 \times 10^6$  BM MNC from unirradiated mice and mice at days 1, 3, 7, 14 and 28 after TBI were cultured in T25 flasks for 9 days and the absolute number of CFU-F contained in two hind legs were counted. The data are expressed as means±SD (n=3). \*\* $p < 0.01$  vs. control.

customized mouse whole body software package (DMS, Montpellier, France) according to the recommended procedure.

### Statistical analysis

Data are expressed as the mean±standard deviation (SD) for separate experiments and were analyzed by ANOVA or Student's t test as appropriate, with  $p < 0.05$  considered statistically significant.

## Results

### TBI reduced the pool of BM mesenchymal stem/progenitor cells

In a preliminary study, we found that exposure of mice to increasing doses of TBI (2, 4, 6.5 and 8 Gy) led to reduction in the number of BM MNC and the frequencies of CFU-F in a dose- and time-dependent manner (*data not shown*). To further characterize the effects of TBI on BM MSC, mice were exposed to a single dose of 4 Gy of TBI. Changes in the number of BM MNC and frequencies of CFU-F were monitored for up to 4 weeks after TBI. Exposure to 4 Gy TBI resulted in an immediate decrease in the number of BM MNC with the nadir occurring at day 3 after TBI. Thereafter, the number of BM MNC recovered gradually, and almost returned to the normal level by day 28 after TBI (*Supplementary Figure 1A*). Surprisingly, the frequency of CFU-F per  $10^6$  BM MNC reached a maximum on day 3, and then diminished gradually over the subsequent 3.5 weeks (*Supplementary Figure 1B*). As irradiation had resulted in a hypocellular BM and rapid reduction in the number of BM MNC, we then analyzed the absolute number of CFU-F contained in the hind legs of individual mice. After TBI, the absolute number of CFU-F decreased immediately and sharply, recovered slightly by day 3, and then gradually declined over the subsequent 3.5 weeks (Figure 1). The frequency of CFU-F at day 28 accounted for only 7% of that in normal control mice, indicating the shrinking pool of BM mesenchymal stem/progenitor cells after TBI.

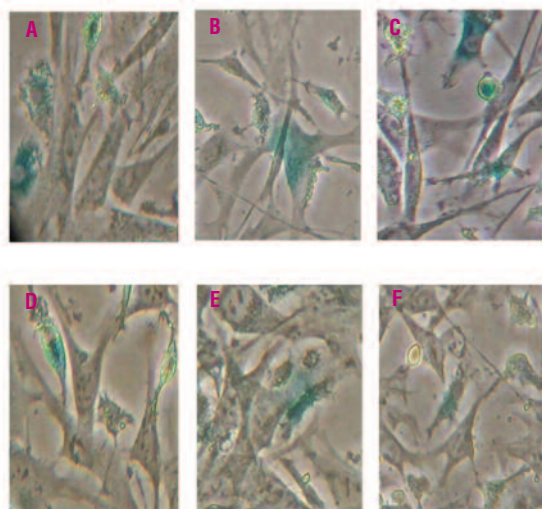


**Figure 2.** TBI did not increase SA- $\beta$ -gal activity in BM MSC. Representative SA- $\beta$ -gal staining of BM MSC isolated from control mice (A) and mice 1 (B), 3 (C), 7 (D), 14 (E) and 28 (F) days after TBI. Microphotographs were taken at 200 $\times$  magnification.

### TBI did not induce changes in morphology or SA- $\beta$ -gal activity of BM MSC related to cellular senescence

Evidence from both *in vitro* culture systems and murine models has indicated that senescence in HSC contributes to the latent damage to hematopoietic function.<sup>5,6</sup> This prompted us to determine whether TBI resulted in cellular senescence in BM MSC. Aged MSC are reportedly larger, have more podia, and show a more flattened morphology than their younger counterparts.<sup>16,17</sup> In our study, cultured BM MSC derived from mice that had or had not been irradiated all showed spindle-like morphology, were similar in cell size, and did not have a significantly enlarged or flattened morphology (Figure 2A-F). Moreover, TBI did not affect colony size (*data not shown*), which is not consistent with the finding previously reported that the average colony size decreases in aged MSC.<sup>18,19</sup> Finally, we did not detect any increase in the activity of SA- $\beta$ -gal – a widely used biomarker of cellular senescence<sup>20</sup> – as a result of TBI (Figure 2 and *Supplementary Figure 2*).

### TBI did not induce cell cycle arrest

Other salient features of cellular senescence are irreversible growth arrest in the G<sub>1</sub> phase of the cell cycle and an impairment of proliferation potential. In our study, we conducted cell cycle analysis for D0, D3, D7, D14 and D28. Under normal conditions, 86.1 $\pm$ 2.64% of BM MSC were in the G<sub>0</sub>/G<sub>1</sub> phase. We found that TBI did not induce G<sub>1</sub> arrest. At day 3 after TBI, an increased proportion of cells entered the S phase ( $p=0.002$ ) and the level returned to normal at day 28. The difference in cell cycle distribution of D0 and D14 or D28 was not statistically significant. This result indicates that TBI did not induce cell cycle arrest in BM MSC, and, on the contrary, stimulated their proliferation transiently in the acute phase after injury (day 3).

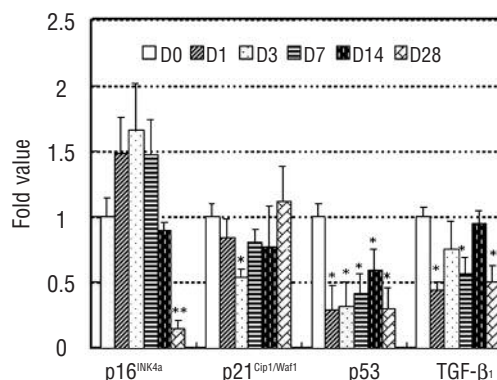


**Figure 3.** TBI did not increase the expression of senescence related genes in BM MSC. At 1, 3, 7, 14 and 28 days after 4Gy TBI, BM MSC were cultured as mentioned above. The mRNA expression for p16<sup>INK4a</sup>, p21<sup>waf1</sup>, p53 and TGF- $\beta$  1 were analyzed by real-time RT-PCR with  $\beta$ -actin as the internal control. Fold expression values were normalized to BM MSC derived from unirradiated mice. No significant increase in the levels of these genes were observed. Data are expressed as means $\pm$ SD of three independent experiments \* $p<0.05$  and \*\* $p<0.01$  vs. BM MSC derived from unirradiated mice.

### TBI did not increase the expression of genes related to cellular senescence

Several studies have suggested that cellular senescence is accompanied by changes in expression of genes such as inhibitors of cyclin-dependent kinases, p16<sup>INK4a</sup>, p21<sup>waf1</sup>, and p53.<sup>5,6,21</sup> In addition, there is evidence of the involvement of TGF- $\beta$ 1 in cellular senescence.<sup>22,23</sup> In this study, we examined the expression of these genes in BM MSC by real-time reverse transcriptase RT-PCR for any molecular signatures of senescence as a result of TBI. As shown in Figure 3, although the expression of p16<sup>INK4a</sup> mRNA increased slightly in the D3 group (1.47-1.66 fold increase), no statistically significant difference was observed. After the transient increase, p16<sup>INK4a</sup> mRNA expression reduced greatly in the D28 group (0.15 fold that of normal controls). The mRNA expression of p21<sup>waf1</sup>, p53 and TGF- $\beta$ 1 did not increase during the observation either. These results, along with the other findings mentioned above, indicate that TBI did not induce cellular senescence in BM MSC, at least at the dose of TBI used and based on the senescence markers examined.

### TBI altered the osteogenic potential of BM MSC

Although there was no evidence of senescence, the osteoblast differentiation potential of BM MSC was obviously altered as a result of TBI. BM MSC isolated from mice at various time points after TBI were transferred to an osteogenic medium for 1 or 3-week induction followed by the examination of ALP activity and mineral deposition, the hallmarks of bone formation. As shown in Figure 4, shortly after irradiation (days 1 and 3), the osteogenic differentiation potential increased significantly, with more ALP-positive cells after 1 week of culture in osteogenic medium (Figure 4A) and a calcium-rich mineralized matrix in the induction dish after 3 weeks of induction

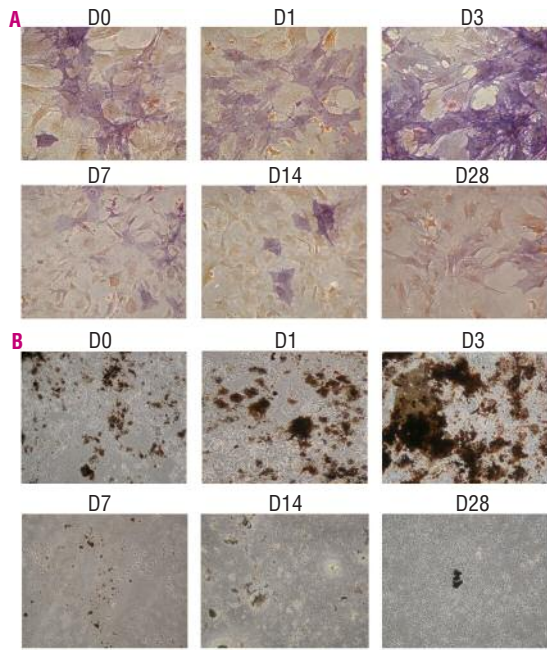


**Figure 4.** TBI altered the osteogenesis potential of BM MSC *in vitro*. BM MSC from mice with or without 4 Gy TBI were cultured and then induced for osteogenic differentiation *in vitro*. **A.** Alkaline phosphatase staining was performed at the end of 1 week of the osteogenic differentiation, the differentiated BM MSC positive for alkaline phosphatase were stained purple. **B.** After 3 weeks' induction, Von Kossa staining was performed, the induced cells showed calcium accumulation. Microphotographs were taken at 100 $\times$  magnification.

(Figure 4B). However, the enhanced differentiation potential decreased sharply in the D7 group, with no marked recovery up to the D28 group. These results indicate that the long-term osteoblast differentiation potential might be compromised. By using highly sensitive real-time RT-PCR, we found that expression of some osteogenesis-related genes in BM MSC was altered after 1 and 3 weeks of culture in the osteogenic medium. As shown in Figure 5A and B, treating mice with a single dose of TBI led to phase-dependent changes in all the genes examined. After 1 week of osteogenic induction, early phase of osteoblast differentiation, core-binding factors 1 (Cbfa1), type 1 collagen and osteocalcin showed highest expression in D3 and reached the nadir in D28. The expression of osteopontin also peaked in D3 with no significant difference at other time points. These results indicate that D3 had more powerful osteogenic potential. Cbfa1 is necessary for osteoblast differentiation and its expression is maintained postnatally in fully differentiated osteoblasts.<sup>24</sup> At the end of 3 weeks of culture in osteogenic medium, osteoblast differentiation should be characterized by mineralization of the mature matrix. At this time point, the expression of Cbfa1 was again highest in D3 but the expression of type 1 collagen and osteocalcin, the markers of the early phase of osteoblast differentiation and differentiated osteoblasts, respectively, was highest in D28 and lowest in D3. Meanwhile, the effect of TBI on the mRNA expression of osteopontin, another marker of bone extracellular matrix,

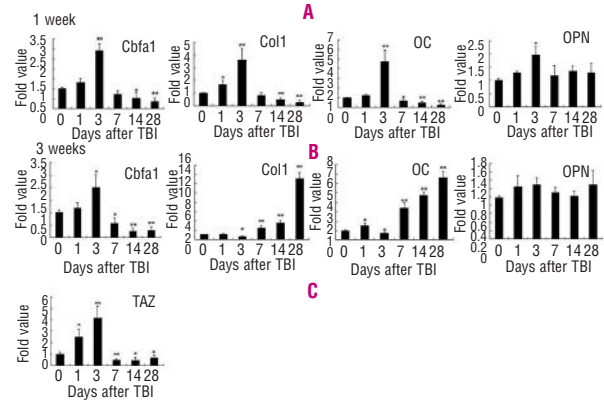


**Figure 5.** TBI altered mRNA expression of osteoblast-related genes. Total RNA was extracted from BM MSC induced in osteogenic differentiation medium for 1 or 3 weeks. After 1 or 3 weeks of osteogenic induction, the expression of genes of interest was normalized to  $\beta$ -actin expression and given as a fold value: **A.** The change in mRNA expression of Cbfa1, osteocalcin, type 1 collagen and osteopontin after 1 week of induction. **B.** The change in mRNA expression of Cbfa1, osteocalcin, type 1 collagen and osteopontin after 3 weeks' induction. **C.** For detection of TAZ expression, the total RNA was extracted from BM MSC at different time points after TBI without osteogenic differentiation. Graphs represent means $\pm$ SD of three independent experiments \*,  $p < 0.05$  and \*\* $p < 0.01$ .

was not significant after 3 weeks of induction. All these results indicate that, following transient enhanced osteogenic potential (D3), the osteoblast differentiation from BM MSC may be defective (D7-D28).

#### TBI altered the expression of TAZ before osteogenic induction of BM MSC

TAZ (transcriptional coactivator with PDZ-binding motif) functions as a transcriptional modulator to stimulate bone development (versus adipogenesis) of MSC through co-activation of Cbfa1-dependent gene transcription.<sup>25</sup> Here we examined whether the alteration of the osteogenic differentiation potential of BM MSC caused by TBI is due to changes in TAZ expression, which might have occurred before osteogenic induction. Real-time RT-PCR analysis showed that the expression of TAZ mRNA in BM MSC from irradiated mice was initially increased (2.49-fold on day 1 and 4.16-fold on day 3 after TBI), but was reduced greatly from day 7 to day 28 after TBI (Figure 5C). The changes in TAZ expression in BM MSC were consistent with this following *in vitro* induction.

#### The effect of TBI on osteoblasts, trabecular structure, osteoid and BMD

As the osteogenic differentiation potential of BM MSC was impaired *in vitro* as a result of TBI, we wondered whether there are corresponding bone changes *in vivo*. In the control mice, osteoblasts were tightly packed along the surface linings of bone (Figure 6 A,B), and both the osteoblasts and osteoid were obvious with osteoblasts sinking down into the osteoid (Figure 7A, B). By contrast, the TBI-treated mice showed a progressive decrease in the number of osteoblasts (Figure 6, 7A-D A-D and G). At day 28 after TBI, osteoblasts were detectable only on the sur-

face of trabecular bone, rather than existing along the long bone (Figures 7 C and D), and the number of osteoblasts per section was reduced to only 38.1% of that of normal mice (Figure 7G). These results are in line with an *in vitro* defect in osteoblast differentiation and maturation.

In addition, we also noted that the trabecular structure was gradually fragmented (Figure 6), especially at day 28. In clinical practice, atrophy of the trabeculae bone, osteopenia and osteoporosis are complications in survivors of childhood or adult cancer who receive different doses of irradiation.<sup>26</sup> Using DEXA, currently the best referenced method for examining bone mass, we found no difference in BMD between irradiated mice and their control littermates at 4 weeks after 4 Gy TBI; however, at 15 weeks after TBI, irradiated mice had decreased total BMD ( $p < 0.05$ ) (Figure 7I). This indicates that irradiated mice had significant bone loss and were prone to osteoporosis.

### The effect of TBI on the osteoblastic niche for hematopoiesis

A subset of osteoblasts, SNO, has recently been characterized as a key cellular component of the HSC niche.<sup>15</sup> Here we examined whether the impairment of osteogenesis had an effect on the hematopoietic niche. SNO and N-cadherin<sup>+</sup> larger, oval-shaped, matrix-forming osteoblasts normally co-exist in BM (Figure 7E). At day 28 post-TBI, osteoblasts as well as SNO decreased significantly (Figure 7F, H). These results imply that exposure to TBI can cause long-term damage to the HSC niche, probably resulting from defective osteogenic potential of BM MSC.

## Discussion

In this study, using a murine TBI model, we found that exposure to a moderate dose of TBI significantly reduced the pool of bone marrow stem/progenitor cells and altered osteogenic potential of BM MSC. However, there was no cellular/molecular evidence of senescence in BM MSC.

The number of CFU-F is a measure to quantify the total number of mesenchymal stem/progenitor cells.<sup>27</sup> Therefore, the significant reduction in CFU-F is a reflection of reduction in the mesenchymal stem/progenitor cell pool as a result of TBI. Although annexin V staining – a method used to detect the early phase of apoptosis – did not show a significant presence of apoptosis in BM MSC (the first three passages were checked, *data not shown*), we cannot exclude the possibility that apoptosis of BM MSC occurred *in vivo* immediately after TBI. As self-renewal is important for the maintenance of the stem cell pool and defective BM MSC self-renewal can lead to a reduction in CFU-F,<sup>28</sup> we infer that the machinery of self-renewal of BM MSC might have been injured during TBI, which deserves further investigation. It has been reported previously that irradiation can lead to cellular senescence in HSC, resulting in compromised self-renewal of HSC and shrinkage of the HSC pool.<sup>5,6</sup> However, based on the studies of morphology, cell cycle analysis, SA-

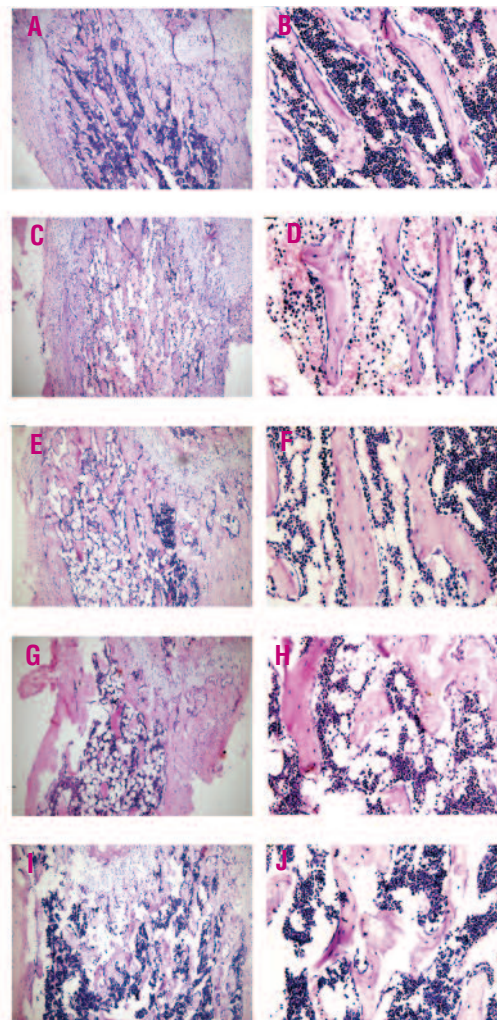


**Figure 6.** Progressive alteration of osteoblasts and trabecular bone in mice that received 4Gy irradiation. Representative hematoxylin and eosin staining of sections of decalcified femora from control mice (A and B) and mice 3 (C and D), 7 (E and F), 14 (G and H) and 28 days (I and J) after TBI. Magnifications: A, C, E, G and I 100 $\times$ ; B, D, F, H and J 400 $\times$ .

$\beta$ -gal activity and senescence-related gene expression, we found no evidence of senescence in BM MSC. These data indicate that irradiation-mediated shrinkage of the mesenchymal stem/progenitor cell pool was independent of cellular senescence.

Active osteoblasts have high expression of ALP and only fully mature osteoblasts can produce a matrix that is subsequently mineralized. Thus, the results of ALP histochemistry, Von Kossa staining as well as changes in mRNA expression of osteoblastic markers suggest TBI may alter the osteoblast differentiation program. *Cbfa1* is a differentiation regulator in the osteoblast lineage and crucial for regulating the rate of bone matrix deposition by differentiated osteoblasts.<sup>29,31</sup> In the osteogenic induction culture, the changes in *Cbfa1* expression in BM MSC were consistent with the results of ALP and Von Kossa staining and also the altered osteogenesis capacity of BM MSC after irradiation. Type 1 collagen is an early marker of osteoblast differentiation, which is induced early and declines as the matrix dep-

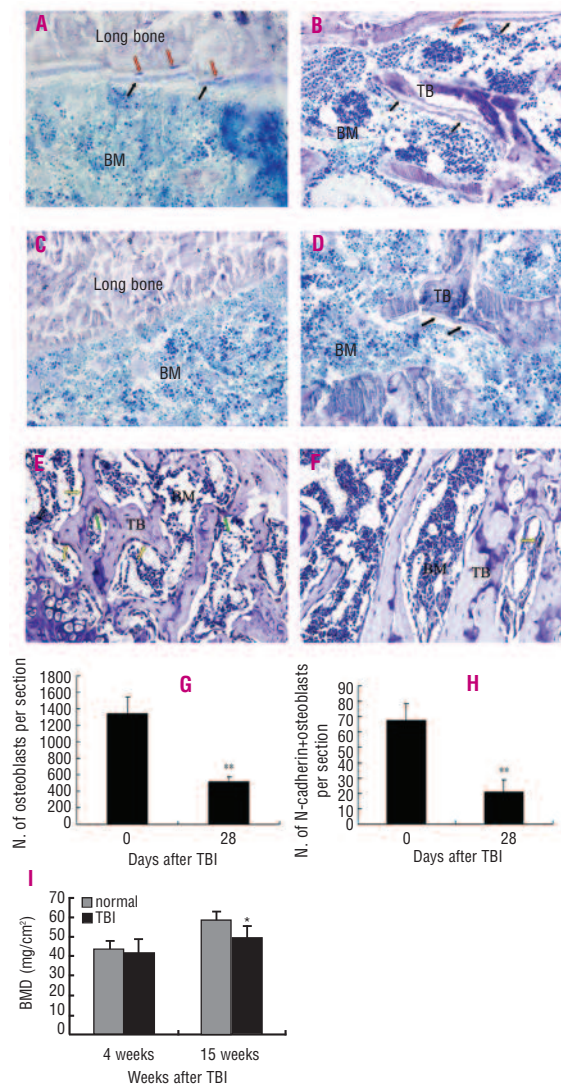


**Figure 7.** The effect of TBI on osteoblasts, osteoid and SNO. (A-D). Photomicrographs of undecalcified murine femoral sections stained with toluidine blue (400 $\times$ ). Osteoid existing between the osteoblast and bone is light blue and mineralized bone is light purple. There is a row of osteoblasts (indicated by black arrows in A, B and D) lining the osteoid seam. Red arrows in A and B indicate the osteoblast cells that are being trapped in lacunae within the matrix of bone as osteocytes. E, F. Representative photomicrographs of immunohistochemical staining of decalcified femoral sections with N-cadherin (normal and 28 days after TBI, respectively). The yellow arrows in E and F indicate positive brown staining in SNO whereas the green arrows indicate that in matrix-forming osteoblasts. Magnifications, 400 $\times$ . (G and H): Bar graphs of the number of osteoblasts (G) and SNO (H) in control and mice that received 4Gy TBI. I. DEXA analysis of total body BMD in irradiated mice and their control unirradiated littermates (n=5/group). A statistically significant difference in BMD was observed at 15 weeks after 4 Gy TBI, whereas no significant difference existed at 4 weeks after TBI. The data are presented as mean $\pm$ SD. \* $p$ <0.05, \*\* $p$ <0.01.

osition phase nears completion.<sup>32</sup> Osteocalcin is a marker expressed only by fully differentiated osteoblasts,<sup>33</sup> and is absent at the terminal stage of osteoblast differentiation, namely the differentiation of osteoblasts to lining cells and osteocytes. Osteopontin is first expressed during the period of active cell proliferation, decreases post-proliferatively, and then increases again at the onset of mineralization, to achieve peak levels during mineralization.<sup>34</sup> Surprisingly, we

found that the expression of type 1 collagen and osteocalcin was consistent with Cbfa1 expression and the osteogenesis capacity of BM MSC after 1 week of osteogenic induction but inversely correlated with them after 3 weeks of culture in osteogenic medium. Since these genes play specific roles in osteogenesis, we speculate that the osteoblast differentiation process had been altered, being accelerated in the early phase (day 3) and delayed thereafter.

Although there is a report that MSC lose osteogenic potential with aging, no definite statement regarding age-related effects on differentiation potential can be made.<sup>35</sup> Furthermore, we found no evidence of cellular senescence in BM MSC in our study, thus we consider that the impediment to osteogenic differentiation and maturation is unrelated to cellular senescence. Osteoblasts originate from BM MSC and Cbfa1 is a key transcription factor for driving MSC to differentiate into osteoblasts. Consequently, as a regulator of Cbfa1, TAZ functions as a molecular rheostat regulating MSC differentiation.<sup>25</sup> The changes in TAZ expression in BM MSC before osteogenic induction imply that irradiation might have damaged the pathway of osteodifferentiation, which requires further investigation. Our results indicate that changes in osteogenesis could be a secondary effect of irradiation-induced damage to BM MSC.

Bone loss and other bone complications as a result of irradiation have been evidenced in murine models<sup>36</sup> and clinical work.<sup>10,26</sup> Regulation of the bone volume, particularly under pathological conditions, is dependent not only on the pathways that mediate terminal differentiation of bone cells, but also on the availability of stem cells for allowing the differentiation to occur.<sup>37</sup> In fact, there are reported cases of osteoporosis associated with stem-cell defects.<sup>28</sup> Here, we postulate that the reduced quantity of and impaired osteogenic potential in BM MSC might be the underlying cause of bone loss as a result of TBI. Furthermore, it has yet to be determined whether TBI causes changes in osteoclast precursors, which in turn affect the number and activities of osteoclasts that are responsible for bone reabsorption.

The close relationship between osteogenesis and hematopoiesis, as well as the involvement of osteoblasts in the regulation and/or maintenance of HSC *in vivo*, has recently been documented by many studies.<sup>15,38,39</sup> Zhang *et al.*<sup>15</sup> has further demonstrated that a subset of SNO fulfill the function of an osteoblastic niche for hematopoiesis and suggested that N-cadherin-expressing HSC are anchored to SNO via N-cadherin-mediated homotypic interactions. In this study, we evaluated the effect of TBI on the hematopoietic niche by examining the changes in SNO, and found that the number of SNO was reduced greatly at day 28 after TBI, implying a significant shrinkage of the size of the osteoblastic niche in BM. These data suggest that, in addition to defects in HSC, damage to the hematopoietic niche could also contribute to the long-term hematopoietic injury. Consistent with our results, Visnjic *et al.*<sup>39</sup> reported that, in mice in which osteoblasts were conditionally ablated by targeting expression of thymidine kinase (which induces cell death in response to ganciclovir), progressive bone loss

was accompanied by a decrease in BM cellularity, including a decrease in the number of Lin-Sca-1<sup>+</sup>c-Kit<sup>+</sup> HSC. Although the complications following irradiation therapy have been noted in a clinical setting, the inter-related factors complicate the interpretation. Using a murine TBI model, we explored the mechanism at the BM MSC level. Our study has shown that shrinkage of the mesenchymal stem/progenitor cell pool and impairment of osteogenic potential take place in BM MSC after TBI, and that these effects occur through a senescence-independent mechanism. Our results suggest that these changes in BM MSC might be primary factors responsible for long-term bone loss and also partially contribute to hematopoietic injury after TBI.

## References

- Domen J, Gandy KL, Weissman IL. Systemic overexpression of BCL-2 in the haematopoietic system protects transgenic mice from the consequences of lethal irradiation. *Blood* 1998;91:2272-82.
- Meng A, Wang Y, Brown SA, Van Zant G, Zhou D. Ionizing radiation and busulfan inhibit murine bone marrow cell haematopoietic function via apoptosis-dependent and -independent mechanisms. *Exp Hematol* 2003;31:1348-56.
- Lohrmann H, Schreml W. Long-term haematopoietic damage after cytotoxic drug therapy for solid tumors. In: Testa NG, Gale RP, eds. *Haematopoiesis-Long-term effects of chemotherapy and radiation*. New York: Marcel Dekker, Inc.; 1988:325-37.
- Testa NG, Hendry JH, Molineux G. Long-term bone marrow damage in experimental systems and in patients after radiation or chemotherapy. *Anticancer Res* 1985;5:101-10.
- Meng A, Wang Y, Van ZG, Zhou D. Ionizing radiation and busulfan induce premature senescence in murine bone marrow haematopoietic cells. *Cancer Res* 2003; 63:5414-9.
- Wang Y, Schulte BA, LaRue AC, Ogawa M, Zhou D. Total body irradiation selectively induces murine haematopoietic stem cell senescence. *Blood* 2006; 107: 358-66.
- Wang X, Hisha H, Taketani S, Adachi Y, Li Q, Cui W, et al. Characterization of mesenchymal stem cells isolated from mouse fetal bone marrow. *Stem Cells* 2006; 24:482-93.
- Short B, Brouard N, Occhiodoro-Scott T, Ramakrishnan A, Simmons PJ. Mesenchymal stem cells. *Arb Med Res* 2003;34: 565-71.
- Muguruma Y, Yahata T, Miyatake H, Sato T, Uno T, Itoh J, et al. Reconstitution of the functional human haematopoietic microenvironment derived from human mesenchymal stem cells in the murine bone marrow compartment. *Blood* 2006; 107: 1878-87.
- Galotto M, Berisso G, Delfino L, Podesta M, Ottaggio L, Dallorso S, et al. Stromal damage as consequence of high-dose chemo/radiotherapy in bone marrow transplant recipients. *Exp Hematol* 1999; 27:1460-6.
- Fang B, Shi M, Liao L, Yang S, Liu Y, Zhao RC. Systemic infusion of Flk1<sup>+</sup> mesenchymal stem cells ameliorate carbon tetrachloride-induced liver fibrosis in mice. *Transplantation* 2004; 78: 83-8.
- Fang B, Shi M, Liao L, Yang S, Liu Y, Zhao RC. Multiorgan engraftment and multilineage differentiation by human fetal bone marrow Flk1<sup>+</sup>/CD31-CD34-progenitors. *J Hematother Stem Cell Res* 2003; 12:603-13.
- Cao Y, Sun Z, Liao L, Meng Y, Han Q, Zhao RC. Human adipose tissue-derived stem cells differentiate into endothelial cells in vitro and improve postnatal neovascularization in vivo. *Biochem Biophys Res Commun* 2005;332: 370-9.
- Li J, Shi M, Cao Y, Yuan W, Pang T, Li B, et al. Knockdown of hypoxia-inducible factor-1 alpha in breast carcinoma MCF-7 cells results in reduced tumor growth and increased sensitivity to methotrexate. *Biochem Biophys Res Commun* 2006; 342:1341-51.
- Zhang J, Niu Ch, Ye L, Huang H, He X, Tong WG, et al. Identification of the haematopoietic stem cell niche and control of the niche size. *Nature* 2003; 425: 836-41.
- Baxter MA., Wynn RF, Jowitt SN, Wraith JE, Fairbairn LJ, Bellantuono I. Study of telomere length reveals rapid aging of human marrow stromal cells following in vitro expansion. *Stem Cells* 2004;22:675-82.
- Mauney JR, Kaplan DL, Volloch V. Matrix-mediated retention of osteogenic differentiation potential by human adult bone marrow stromal cells during ex vivo expansion. *Biomaterials* 2004;25:3233-43.
- Chen CS. Phorbol ester induces elevated oxidative activity and alkalization in a subset of lysosomes. *BMC Cell Biol* 2002; 3:21.
- Globerson A. Thymocytopoiesis in aging: the bone marrow-thymus axis. *Arch Gerontol Geriatr* 1997;24:141-55.
- Dimri GP, Lee X, Basile G, Acosta M, Scott G, Roskelley C, et al. A biomarker that identifies senescent human cells in culture and in aging skin in vivo. *Proc Natl Acad Sci USA* 1995;92:9363-7.
- Krishnamurthy J, Torrice C, Ramsey MR, Kovalev GI, Al-Regaiey K, Su L, et al. Ink4a/Arf expression is a biomarker of aging. *J Clin Invest* 2004;114:1299-307.
- Frippiat C, Chen QM, Zdanov S, Magalhaes JP, Remaclé J, Toussaint O. Subcytotoxic H<sub>2</sub>O<sub>2</sub> stress triggers a release of transforming growth factor-beta1, which induces biomarkers of cellular senescence of human diploid fibroblasts. *J Biol Chem* 2001;276:2531-7.
- Tremain R, Marko M, Kinnimulki V, Ueno H, Bottinger E, Glick A. Defects in TGF-beta signaling overcome senescence of mouse keratinocytes expressing v-Ha-ras. *Oncogene* 2000; 19:1698-709.
- Ducy P, Zhang R, Geoffroy V, Ridall AL, Karsenty G. *Osf2/Cbfa1*: a transcriptional activator of osteoblast differentiation. *Cell* 1997;89:747-54.
- Hong JH, Hwang ES, McManus MT, Amsterdams A, Tian Y, Kalmukova R, et al. TAZ, a transcriptional modulator of mesenchymal stem cell differentiation. *Science* 2005; 309:1074-8.
- Hopewell JW. Radiation-therapy effects on bone density. *Med Pediatr Oncol* 2003; 41:208-11.
- Prockop DJ. Marrow stromal cells as stem cells for nonhaematopoietic tissues. *Science* 1997;276:71-4.
- Bonyadi M, Waldman SD, Liu D, Aubin JE, Grynaps MD, Stanford WL. Mesenchymal progenitor self-renewal deficiency leads to age-dependent osteoporosis in Sca-1/Ly-6A null mice. *Proc Natl Acad Sci USA*. 2003;100: 5840-5.
- Komori T, Yagi H, Nomura S, Yamauchi A, Sasaki K, Dequchi K, et al. Targeted disruption of *Cbfa1* results in a complete lack of bone formation owing to maturational arrest of osteoblasts. *Cell* 1997; 89: 755-64.
- Otto F, Thornell AP, Crompton T, Denzel A, Gilmour KC, Rosewell IR, et al. *Cbfa1*, a candidate gene for cleidocranial dysplasia syndrome, is essential for osteoblast differentiation and bone development. *Cell* 1997; 89:765-71.
- Ducy P. *Cbfa1*: a molecular switch in osteoblast biology. *Dev Dyn* 2000; 219: 461-71.
- Beck GR Jr, Zerler B, Moran E. Gene array analysis of osteoblast differentiation. *Cell Growth Differ* 2001;12:61-8.
- Castro CH, Shin CS, Stains JP, Cheng SL, Sheikh S, Mbalaviele G, et al. Targeted expression of a dominant-negative N-cadherin in vivo delays peak bone mass and increases adipogenesis. *J Cell Sci* 2004; 117:2853-64.
- de Oliveira PT, Zalzal SF, Irie K, Nanci A. Early expression of bone matrix proteins in osteogenic cell culture. *J Histochem Cytochem* 2003; 51:633-41.
- Sethé S, Scutt A, Stolzing A. Aging of mesenchymal stem cells. *Aging Res Rev* 2006; 5: 91-116.
- Hamilton SA, Pecaunt MJ, Gridley DS, Travis ND, Bandstra ER, Willey JS, et al. A murine model for bone loss from therapeutic and space-relevant sources of radiation. *J Appl Physiol* 2006; 101:789-93.
- Blair HC, Carrington JL. Bone cell precursors and the pathophysiology of bone loss. *Ann N Y Acad Sci* 2006; 1068:244-9.
- Calvi LM, Adams GB, Weibrecht KW, Weber JM, Olson DP, Knight MC, et al. Osteoblastic cells regulate the haematopoietic stem cell niche. *Nature* 2003; 425: 841-6.
- Visnjic D, Kalajic Z, Rowe DW, Katavic V, Lorenzo J, Aguilu HL. Haematopoiesis is severely altered in mice with an induced osteoblast deficiency. *Blood* 2004; 103:3258-64.

## Conflict of Interest

The authors reported no potential conflicts of interest.